Zang, A., Majer, E., Bruhn, D. (2014): Preface. - *Geothermics*, *52*, p. 1-5.

DOI: http://doi.org/10.1016/j.geothermics.2014.07.006

Geothermics 52 (2014) 1-5
doi: 10.1016/j.geothermics.2014.07.006

Preface

1. Introduction

Historic causes of man-made seismicity in the Earth's crust include construction of water-filled dams (class-1), mining operations (class-2), and different energy technologies (class-3). The physics of induced seismicity is related to the redistribution of mechanical stresses, i.e., the perturbation of the in situ state of stress at a given site (*Stephansson and Zang*, 2012) due to human interaction. Since a causal relationship between seismicity and the impoundment of lakes was identified, reservoir-induced seismicity (class-1) has been investigated to study the effect of initial lake filling and water level fluctuations on the crustal stress field (*Talwani and Acree*, 1985). Various aspects of man-made class-1 seismicity are summarized in *Gupta* (2011). A dominating portion of class-2 seismicity is caused by underground rock excavation (i.e., *Cook*, 1976). While stress redistribution in class-1 seismicity is due to the added weight of water, class-2 seismicity is associated with the removal of rock material. Stress concentrations occur in areas around underground openings, leading to fracture initiation and to seismic rock response. In severe cases, rock failure occurs in form of rock bursts and/or Ortlepp shear ahead of tunnel faces (*Ortlepp*, 1997), i.e., in deep South African gold mines (*Mendecki*, 1997). In addition, open pit mines and near-surface engineering projects can suffer from induced seismic events (*Brady and Brown*, 2004). Class-3 seismicity is tied to waste-water injection in boreholes and to withdrawal of fluid and gas from the subsurface. In this issue, injection-induced seismicity is subdivided into oil and gas (class-3a), disposal wells (class-3b), carbon capture and storage (class-3c), and geothermal energy development (class-3d). An early study of deep-well related seismicity based on 46 cases in North America, is presented by *Nicholson and Wesson* (1992). *Phillips et al.* (2002) compared seismicity from hydrocarbon exploration (class-3a) with seismicity from geothermal reservoirs (class-3d). In general, class-3 induced seismicity is thought to result from either stress increase or strength decrease of pre-existing fractures. Among the mechanisms discussed, are hydraulic shear (hydro-shear) caused by pore pressure increase, fluid-volume changes, pressure diffusion or thermal stress changes (*Majer et al.*, 2007). It is not a simple task, however, to identify the actual mechanisms leading to induced seismicity. For example, geothermal seismicity (class-3d) is not exclusively related to thermal stress, and seismicity near brine disposal wells (class-3b) is not exclusively related to the amount of fluid-volume injected. Recently, the risk of class-3d seismicity was addressed by *Giardini* (2009) evaluating the Basel enhanced geothermal system (EGS) site. Subsequently, *Evans et al.* (2012) compiled a survey of induced seismicity responses to fluid-injection in various European geothermal (class-3d) and CO_2 reservoirs (class-3c). A recent systematic review, which focuses on EGS sites is given by *Breede* et al. (2013). While it is well known that conventional and enhanced oil recovery operations are associated with seismic events (class-3a, *Suckale*, 2009), multi-stage hydraulic fracturing in shale gas plays (unconventionals) can also generate induced seismicity. However, the application of hydraulic fracturing to tight shale formations typically induces seismicity with magnitudes too low to be felt by the population (*Warpinski et al.*, 2012). If, however, deep fluid injection wells are communicating with near-by basement faults, seismic magnitudes can increase to levels of felt seismicity (i.e., *Kim*, 2013). These cases of felt seismicity resulting from hydraulic fracturing can be considered both rare and anomalous (*Maxwell*, 2013). However, similar scenarios are discussed in CO_2 sequestration in close proximity to faults (*Mazzoldi et al.*, 2012) and can be of importance in geothermal operations. Injection-induced seismicity (class-3) is steadily increasing because there have been more human operations generating induced seismicity. As pointed out by *Ellsworth* (2013), analyzing cumulative $M > 3$ class-3 events in the mid-continental United States from 1967 to 2012, the steady rate from 1967 to 2000 (21 events per year) increased starting in 2001 and peaked at 188 class-3 induced events per year in 2011. While the emphasis of the review article by *Ellsworth* (2013) centers on class-3b seismicity in terms of scientific understanding, key challenges and hazard assessment, individual event classes of injection-induced seismicity deserve individual investigations.

2. This issue

Among the more notable published compilations on "Induced Seismicity" are the edited volumes by *Trifu* (2002, 2010) and *Cornet* (2007). The focus of this special issue is on geothermal seismicity (class-3d), i.e., seismic events related to the development, stimulation and operation of a geothermal field (particularly in EGS stimulation). In November 2011, the idea for such an issue was launched at the Zurich geothermal week during the discussion on the progress towards understanding induced seismicity in the framework of the European Union funded GEISER project. GEISER stands for geothermal engineering integrating mitigation of induced seismicity in reservoirs, and is aimed at understanding and mitigating induced seismicity in geothermal engineered reservoirs. The overall goal of the project is to improve the technique of EGS by investigating the role of induced seismicity as an instrument to image

fluid pathways generated by multiple hydraulic stimulation treatments and by addressing the consequences of treatments for potential seismic hazard (*Bruhn et al.*, 2011). GEISER was developed with the goal to provide strategies for managing and minimizing the potential for significant injection-induced seismicity during the life of geothermal reservoirs.

In the opening article, *Zang et al.* (2014), present an introduction for part I (site-specific geothermal seismicity, faults and stress) and part II (maximum observed seismic magnitude, modelling induced seismicity and pore pressure-stress coupling) of this special issue. Man-made seismicity from different EGS sites (class-3d) is compared to induced seismicity from waste-water disposal wells (class-3b) and seismicity associated with ultra-deep crustal injection experiments (KTB wells). Among the sites discussed in this overview article are Gross Schönebeck and Unterhaching (Germany), Soultz-sous-Forets (France), Basel (Switzerland), Hengill (Iceland), Berlin (El Salvador), The Geysers (USA) and Paralana (Australia). The mechanism leading to larger magnitude seismic events (LME) is investigated in terms of pore fluid pressure, fluid volume injected and type of reservoir rock. Different approaches (deterministic, probabilistic, empiric) are discussed to estimate the maximum seismic magnitude in a reservoir. A synoptic picture of the complex mixed-mode fracture process in crystalline and sedimentary rock is developed.

Grünthal (2014) discusses the occurrence of induced seismicity at sites of geothermal projects (class-3d) in the light of natural tectonic seismicity, and other types of induced events like mining (class-2) or exploitation of coal, rock salt and potash and hydrocarbon (class-3a) in the western part of Central Europe. His generalized conclusion from rate and magnitude-frequency distribution analysis of events is that geothermal seismicity is minor compared to other types of seismicity in this region.

Megies and Wassermann (2014) investigate induced seismicity in the North Alpine Foreland Basin, in particular in relation to a geothermal plant in the greater Munich area, Unterhaching (Germany). Their conclusion is that non-pressure-stimulated geothermal plants can also produce geothermal seismicity in tectonic settings with previously known low seismic hazard.

Calò et al. (2014) relocate induced seismic events from two hydraulic stimulation campaigns at the Soultz-sous-Forêts, France, EGS site. The comparison of the 2004 and 2005 injection-induced seismic event clouds shows that first, the in situ stress field in the reservoir is not fully restored before the start of the second stimulation, and second, that the mechanism of induced seismic events changed from first to second stimulation.

This is followed by three articles on the analysis of induced seismicity at the Basel (Switzerland) EGS site. Using exclusively data from six borehole seismometers, *Kraft and Deichmann* (2014) found highly similar seismic events during the massive fluid injection test. High-precision seismic hypocenters reveal the fine structure of a complex fault zone rather than a single fault at Basel EGS site.

Zhao et al. (2014) present the results of a moment tensor inversion of seismic events with local magnitude between 2.0 and 3.4 from the same massive stimulation test at the Basel site. The main findings include that events with significant isotropic components occur mainly in the injection phase while post-stimulation events are predominantly pure shear and are located further away from the injection well.

In line with the fact that many of the observed seismic events during the Basel massive stimulation form clusters of similar events (*Kraft and Deichmann*, 2014), *Deichmann et al.* (2014) found that several focal mechanisms of events with local magnitudes between 0.7 and 3.4 are nearly identical to each other. In some cases, the spatial extent of the individual clusters is limited to a few meters suggesting repeated slip with partial stress drop as pore pressure increases. In other cases, that include stronger events with local magnitude above 2, the dimension of individual clusters can amount to several 100 m and the activity within these clusters can extend over several days. The orientation of many fault segments identified in this way deviates significantly from the overall orientation of the seismic cloud.

Kwiatek et al. (2014) analyzed the seismic activity monitored during three different hydraulic stimulation phases at Berlin Geothermal Field, El Salvador. Refinement of event locations by the double-difference technique and refinement of seismic source parameters through spectral ratio method allow (a) to observe the Kaiser effect at shallow and deeper stimulation stages, (b) to interpret the seismic event cloud with respect to the fault system and to the direction of maximum in situ stress and (c) to identify an increase in the static stress drop values with increasing distance from the injection point. While shallow injections display clear alignment with the existing fault system, the deep injection induced seismic events are not related to any pre-existing fault. The refined results do not provide any evidence that the multiple stimulations triggered the moment magnitude 3.6 event recorded two weeks after the second stimulation.

Gritto and Jarpe (2014) use a 34-station seismic geophone net-work at The Geysers geothermal field (California, USA) and analyze seismicity from 2004 to 2011 to correlate the P- and S-wave velocity ratio to the total volume of injected water. The results suggest that over the investigated time period, the fluid saturation has been successfully increased throughout the reservoir.

Part I of this issue closes with a case study on induced seismicity associated with the virgin stimulation phase of the Paralana geothermal field, Australia. *Albaric et al.* (2014) analyzed more than 7000 seismic events during the 2011 stimulation of the well Paralana 2 with about 3 million liters of water to create a geothermal reservoir. Relocated seismic events outline NNE-SSW and ENE-WSW structures that resemble an en echelon fracture network. This finding is in line with the complex fault structure revealed at Basel EGS site (*Kraft and Deichmann*, 2014). The four largest events at Paralana occur during fluid injection, i.e., three events with moment magnitude 2.4 and one event with moment magnitude 2.5.

Geothermics 52 (2014) 1-5
doi: 10.1016/j.geothermics.2014.07.006

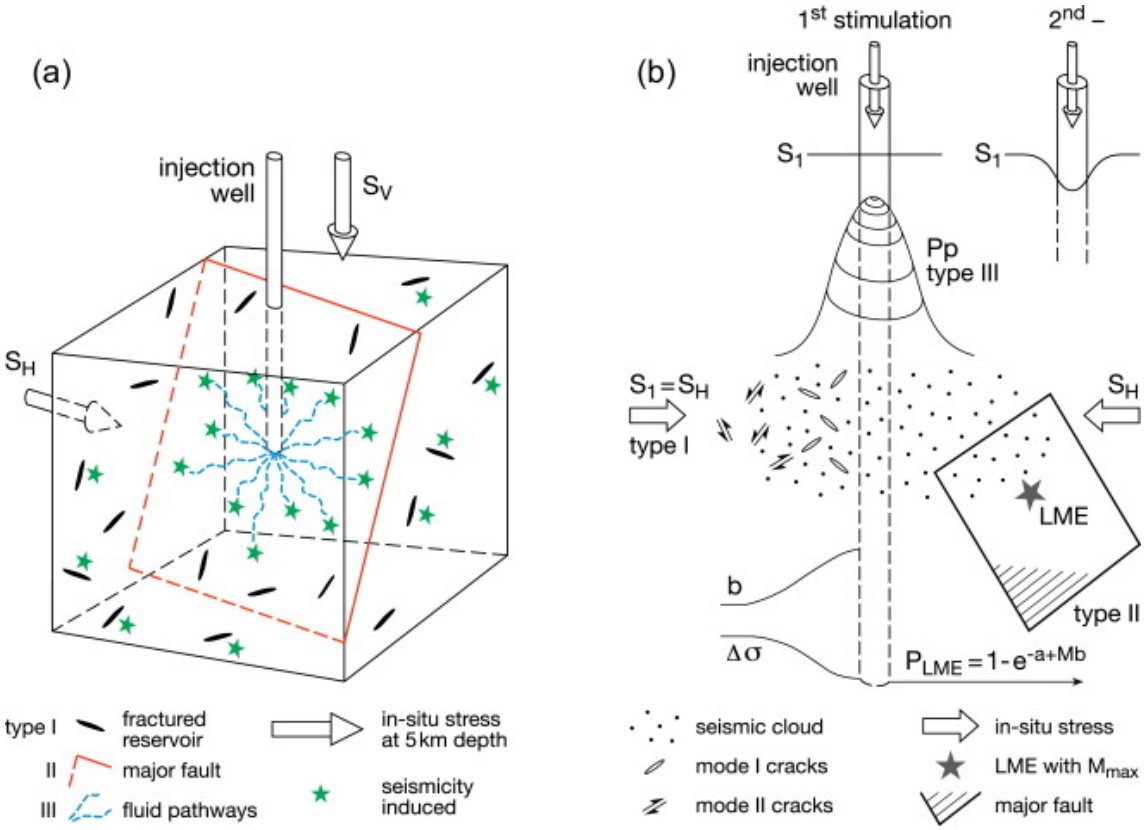

Figure 1. (a) Synoptic picture of three types of key parameters in fractured geothermal reservoir (rock cube 1 km³ in size) at 5 km depth: stress field (arrows), major fault (red plane) and hydraulic energy pumped into the system (blue fluid pathways). Fluid-induced seismicity (green stars) allows to investigate the interplay of key reservoir parameters. (b) Schematic behavior of reservoir parameters with distance from the injection well (near-field). In situ stress $S_1 = S_H$ can change from first to subsequent stimulations and may not fully recover (inset, 2nd stimulation). Pore pressure p_p diffusion is negatively correlated to Brune stress drop, $\Delta\sigma$ and positively correlated to Gutenberg–Richter b-values. Moment tensor inversions of induced seismicity indicate isotropic components (mode I cracks) near well and double-couple components (mode I cracks) further away from the injection well. (For interpretation of the references to color in this figure legend, the reader is referred to the web version of the article.)

Articles in part II are concerned with magnitude scaling, estimating the expected maximum magnitude in the reservoir, modelling of fluid-induced seismicity and pore pressure stress coupling as well as fault and stress control in gas depletion induced seismicity.

Edwards and Douglas (2014) present a magnitude-homogenization exercise for several GEISER datasets of induced seismicity. The results show that homogeneous computation of moment- and local magnitude is useful in hazard assessment of EGS sites. The analyzed data fall into two subsets with well-defined relation to moment magnitude: Basel (Switzerland), The Geysers (USA) and Hengill (Iceland) in one, and Soultz-sous-Forêts (France) and Roswinkel (The Netherlands) gas depletion in another, indicating different source or attenuation properties between the sites within each subset.

Based on Soultz-Sous-Forêts EGS data, *Baujard et al.* (2014) present an heuristic approach for estimating the total seismic moment and the value of the maximum moment magnitude released in a single seismic event occurring during, or after stimulation. The first approach assumes a linear relationship between the pumping energy and the total seismic moment. For a given pumping scheme, a prediction of the total seismic moment is obtained through Gutenberg–Richter relation. The second approach assumes constant values of well injectivity and reservoir hydraulic diffusivity during injection. The energy stored in the reservoir is computed from analytical pressure distributions.

Also for the Soultz-sous-Forêts site, *Wassing et al.* (2014) developed a coupled continuum model of fracture reactivation and induced seismicity during enhanced geothermal operations. Seismic events are simulated using a dynamic friction angle smaller than the static friction angle, while post-seismic healing to the static friction angle is allowed. The granitic rock mass is intersected by a fracture zone. The model is used to perform a sensitivity analysis on in situ stress regime, fracture strength and frictional weakening.

Yoon et al. (2014) use a discrete element approach to simulate induced seismicity in intact and naturally fractured geothermal reservoirs. The hydro-mechanical coupled discrete element simulation allows testing of various injection scenarios in a model reservoir with Soultz-sous-Forêts granite properties. Several field observations on induced seismicity phenomena are reproduced including the creation of new fractures, reactivation of pre-existing joints, post-shut-in seismicity and larger magnitude event with non-double-couple source, Kaiser effect and magnitude-frequency distribution. The main conclusion is that cyclic fluid injection lowers the energy radiated from induced seismicity,

which has the potential to mitigate larger magnitude events, in particular in the post shut-in phase of stimulation.

Hakimhashemi et al. (2014) introduce a new approach to translate effective stress changes, caused by EGS operations, into seismicity rate. This approach, in general, requires no induced seismicity data and can be used as a tool to pre-estimate the effect of the EGS activities on the seismicity rate. The two input parameters (background seismicity and stressing rate) can be estimated using available seismic hazard and stress data at a given site. The approach is applied to the Soultz-sous-Forêts EGS site for the injection in GPK4 in 2004. Similar to *Yoon et al.* (2014), the strength of this approach is the capability to a priori test various injection scenarios and their impact on induced seismicity in the geothermal reservoir.

Altmann et al. (2014) investigate the phenomenon of pore pressure-stress coupling and consequences for reservoir stress and fault reactivation. In particular, the authors show that stress changes in long-term production can induce changes in the stress regime and bring other fault systems closer optimal orientation in the locally perturbed stress field.

In the closing article by *van Wees et al.* (2014), the effect of stress state and faults on induced seismicity is investigated in the light of gas depletion (class-3a) in the Netherlands. The main outcome of this study is that seismicity is observed in no more than 15% of these gas fields. Seismicity occurs due to differential compaction, starting after 28% reservoir depletion. Mechanical analysis indicates that most faults are not critically stressed.

The results of this special issue on induced seismicity are summarized in a synoptic picture in Fig. 1 indicating key reservoir parameters as discussed in the GEISER project (Fig. 1a) and their behavior with distance from injection well (Fig. 1b). In Fig. 1a, three key parameters are indicated: type-I stress field (Fig. 1a, arrows), type-II major fault (Fig. 1a, red plane) and type-III hydraulic energy pumped into the reservoir (Fig. 1a, blue pathways). All parameters depend on the actual size and depth of the fractured geothermal reservoir (Fig. 1a, cube with cracks). Induced seismicity (Fig. 1a, green stars) allows investigating the interplay of key reservoir parameters. For this, observed induced events are categorized by hypocenter locations, source mechanisms, Gutenberg–Richter magnitude-frequency distribution (b-value), larger magnitude events (LME) and peak ground acceleration (PGA).

In Fig. 1b, the schematic behavior of some parameters with distance from the injection well is shown. In situ stress (type-I) can change from first to subsequent stimulations, and may not fully recover (Fig. 1b, inset). Pore pressure, p_p diffusion (type-III) is negatively correlated to Brune stress drop, $\Delta\sigma$ values and positively correlated to seismic b-values. This indicates that major faults (type-II) at the boundary of the reservoir, outlined by the extension of the seismic cloud, carry the highest risk/hazard for the maximum magnitude to occur. Note that the extension of the seismic cloud (Fig. 1b, dots) is not necessarily identical to the fracture zone developed during stimulation of the reservoir (Fig. 1b, mode I and II cracks). The extent of the seismic cloud depends on the resolution and sensitivity of the monitoring network. Moment tensor inversion results indicate dominant portion of isotropic components near-well (tensile cracks, mode I) and pure double couple components (shear cracks, mode II) further away from the injection well.

3. Reviewers

This special issue could not have been possible without the effort and expertise of the reviewers of the articles herein. We cordially thank Christopher McDermott, Jonny Rutqvist, Jeoung-Seok Yoon, Douglas S. Dreger, Gisela Viegas, Oliver Heidbach, Thomas Kölbel, Volker Oye, Gary L. Pavlis, Steve E. Ingebritsen, Hiroshi Asanuma, Marco Bohnhoff, Jim Hazzard, Cornelius Langenbruch, Lawrence Hutchings, Carsten Dinske, Stephen J. Oates, James Rut-ledge, Nicholas C. Davatzes, Julian J. Bommer, Christopher Bromley, Keith Evans, Bettina Goertz-Allmann, Roland Gritto, Gillian R. Foulger, Nicholas Deichmann, Gottfried Grünthal, Mike Fehler, Aurelie Guilhem, B.R. Julian, Grzegorz Kwiatek, William Foxall and David Oppenheimer.

Acknowledgements

This work was supported by the European Union funded project GEISER (Geothermal Engineering Integrating Mitigation of Induced Seismicity in Geothermal Reservoirs, FP7-ENERGY-2009-1, Grant agreement no.: 241321-2). We would like to thank the chief-coordinator, Ernst Huenges for fruitful discussions throughout the life span of this project, 2010–2013.

References

Albaric, J., Oye, V., Langet, N., Hasting, M., Lecomte, I., Iranpour, K., Messeiller, M., Reid, P., 2014. Monitoring of induced seismicity during the first geothermal reservoir stimulation at Paralana, Australia. Geothermics 52, 120-131.

Altmann, J., Müller, B.I.R., Müller, T.M., Heidbach, O., Tingay, M.R.P., Weißhardt, A., 2014. Pore pressure stress coupling in 3D and consequences for reservoir stress states and fault reactivation. Geothermics 52, 195-205.

Baujard, C., Schoenball, M., Kohl, T., Dorbath, L., 2014. Large magnitude events during injections in geothermal reservoirs and hydraulic energy: an heuristic approach. Geothermics 52, 140-152.

Brady, B.H.G., Brown, E.T., 2004. Rock Mechanics for Underground Mining. Springer, Dordrecht, The Netherlands.

Breede, K., Dzebiashvili, K., Liu, X., Falcone, G., 2013. A systematic review of enhanced (or engineered) geothermal systems: past, present and future. Geotherm. Energy 1 (4), http://dx.doi.org/10.1186/2195-9706-1-4.

Bruhn, D., Huenges, E., Ágústsson, K., Zang, A., Kwiatek, G., Rachez, X., Wiemer, S., Van Wees, J.-D., Calcagno, P., Kohl, T., Dorbath, C., De Natale, G., Oye, V., 2011. Geothermal Engineering Integrating Mitigation of Induced Seismicity in Reservoirs – The European GEISER Project, vol. 35. Geothermal Research Council (GRC) Transactions, pp. 1623–1626.

Calò, M., Dorbath, C., Frogneux, M., 2014. Injection tests at the EGS reservoir of Soultz-sous-Forêts, seismic response of the GPK4 stimulations. Geothermics 52, 50-58.

Cook, N.G.W., 1976. Seismicity associated with mining. Eng. Geol. 10, 99–122.
Cornet, F.H., 2007. Introduction to the special issue on induced seismicity. Int. J. Rock Mech. Min. Sci. 44, 1077–1078.
Deichmann, N., Kraft, T., Evans, K., 2014. Identification of faults activated during the stimulation of the Basel geothermal project from cluster analysis and focal mechanisms of the larger magnitude events. Geothermics 52, 84-97.
Edwards, B., Douglas, J., 2014. Magnitude scaling of induced seismicity. Geothermics 52, 132-139.
Ellsworth, W.L., 2013. Injection-induced earthquakes. Science 341, http://dx.doi.org/10.1126/science.1225942.
Evans, K.F., Zappone, A., Kraft, T., Deichmann, N., Moia, F., 2012. A survey of the induced seismic responses to fluid injection in geothermal and CO 2 reservoirs in Europe. Geothermics 41, 30–54.
Giardini, D., 2009. Geothermal quake risk must be faced. Nature 426, 848–849.
Gritto, R., Jarpe, S.P., 2014. Temporal variations of V P /V S ratio at the Geysers geothermal field, USA. Geothermics 52, 112-119.
Grünthal, G., 2014. Induced seismicity related to geothermal projects versus natural tectonic earthquakes and other types of induced seismic events in Central Europe. Geothermics 52, 22-35.
Gupta, H.K., 2011. Artificial water reservoir triggered earthquakes. In: Gupta, H.K. (Ed.), Encyclopedia of Solid Earth Geophysics, vol. I. Springer, Dordrecht, The Netherlands, pp. 15–24.
Hakimhashemi, A.H., Schoenball, M., Heidbach, O., Zang, A., Grünthal, G., 2014. Forward modelling of seismicity rate changes in georeservoirs with a hybrid geomechanical–statistical prototype model. Geothermics 52, 185-194.
Kim, W.-Y., 2013. Induced seismicity associated with fluid injection into a deep well in Youngstown, Ohio. J. Geophys. Res. Solid Earth 118, 3506–3518, http://dx.doi.org/10.1002/jgrb.50247.
Kraft, T., Deichmann, N., 2014. High-precision relocation and focal mechanism of the injection-induced seismicity at the Basel EGS. Geothermics 52, 59-73.
Kwiatek, G., Bulut, F., Bohnhoff, M., Dresen, G., 2014. High-resolution analysis of seismicity induced at Berlin geothermal field, El Salvador. Geothermics 52, 98-111.
Majer, E.L., Baria, R., Stark, M., Oates, S., Bommer, J., Smith, B., Asanuma, H., 2007. Induced seismicity associated with enhanced geothermal systems. Geothermics 36, 185–222.
Maxwell, S., 2013. Unintentional seismicity induced by hydraulic fracturing. CSEG RECORDER, 40–49.
Mazzoldi, A., Rinaldi, A.P., Borgia, A., Rutqvist, J., 2012. Induced seismicity within geological carbon sequestration projects: maximum earthquake magnitude and leakage potential from undetected faults. Int. J. Greenhouse Gas Control 10, 434–442.
Megies, T., Wassermann, J., 2014. Microseismicity observed at a non-pressure-stimulated geothermal power plant. Geothermics 52, 36-49.
Mendecki, A.J., 1997. Seismic Monitoring in Mines. Chapman & Hall, London UK, pp. 280.
Nicholson, C., Wesson, R.L., 1992. Triggered earthquakes and deep well activities. Pure Appl. Geophys. 139 (3–4), 561–578.
Ortlepp, W.D., 1997. Rock Fracture and Rockbursts – An Illustrative Study. The South African Institute of Mining and Metallurgy, Johannesburg, pp. 99.
Phillips, W.S., Rutledge, J.T., House, L.S., Fehler, M.C., 2002. Induced microearthquake patterns in hydrocarbon and geothermal reservoirs: six case studies. Pure Appl. Geophys. 159, 345–369.
Stephansson, O., Zang, A., 2012. ISRM suggested methods for rock stress estimation. Part 5: Establishing a model for the in situ stress at a given site. Rock Mech. Rock Eng. 45, 955–969.
Suckale, J., 2009. Induced seismicity in hydrocarbon fields. Adv. Geophys. 51, 55–106.
Talwani, P., Acree, A., 1985. Pore pressure diffusion and the mechanism of reservoir induced seismicity. Pure Appl. Geophys. 122, 947–965.
Trifu, C.I. (Ed.), 2002. The mechanism of induced seismicity. Pure Appl. Geophys. 159 (1–3) (Topical Issue, Birkhäuser, Basel, 617 pp.).
Trifu, C.I. (Ed.), 2010. Monitoring induced seismicity. Pure Appl. Geophys. (Topical Issue, Birkhäuser, Basel).
van Wees, J.-D., Buijze, L., van Thienen-Visser, K., Nepveu, M., Wassing, B.B.T., Orlic, B., Fokker, P.A., 2014. Geomechanics response and induced seismicity during gas field depletion in the Netherlands. Geothermics 52, 206-219.
Warpinski, N.R., Du, J., Zimmer, U., 2012. Measurements of Hydraulic-Fracture-Induced Seismicity in Gas Shales. SPE Production and Operations, pp. 240–252.
Wassing, B.B.T., van Wees, J.-D., Fokker, P.A., 2014. Coupled continuum modeling of fracture reactivation and induced seismicity during enhanced geothermal operations. Geothermics 52, 153-164.
Yoon, J.-S., Zang, A., Stephansson, O., 2014. Numerical investigation on optimized stimulation of intact and naturally fractured deep geothermal reservoirs using hydro-mechanical coupled discrete particles joints model. Geothermics 52, 165-184.
Zang, A., Oye, V., Jousset, Ph., Deichmann, N., Gritto, R., McGarr, A., Majer, E., Bruhn, D., 2014. Analysis of induced seismicity in geothermal reservoirs – an overview. Geothermics 52, 6-21.
Zhao, P., Kühn, D., Oye, V., Cesca, S., 2014. Evidence for tensile faulting deduced from full waveform moment tensor inversion during the stimulation of the Basel enhanced geothermal system. Geothermics 52, 74-83.

Arno Zang*
German Research Center for Geosciences GFZ, Section 2.6 Seismic Hazard and Stress Field, Telegrafenberg, 14473 Potsdam, Germany

Ernest Majer
Lawrence Berkeley National Laboratory, Berkeley, CA 94720, USA

David Bruhn
GFZ, Section 4.1 Reservoir Technology, Telegrafenberg, 14473 Potsdam, Germany

* Corresponding author. Tel.: +49 331 2881325.
E-mail address: zang@gfz-potsdam.de (A. Zang)